10222 *Inorg. Chem.* **2009**, *48*, 10222–10230
DOI: 10.1021/ic901217k

Inorganic Chemistry
Article

Morphology-Controlled Synthesis of Inorganic Nanocrystals via Surface Reconstruction of Nuclei

Guolei Xiang, Jing Zhuang, and Xun Wang*

Department of Chemistry, Tsinghua University, Beijing, 100084, P. R. China

Received June 24, 2009

The growth mechanism of shape-selected synthesis of nanocrystals in all systems can be attributed to an oriented surface assembly process of growth units, in the present of additives or not. In this article, we present an example displaying the influence of the surface reconstruction process of nuclei on the shape-selected growth behaviors of inorganic nanocrystals. The basic principle lies in the sufficient diffusion of growth units on crystal surfaces according to Kossel's growth model. Shape-controlled octahedral and truncated octahedral crystals of zinc tin oxide (ZTO) were successfully synthesized by pretreating precursors at room temperature without any surfactants. And, the method can be applied to $CaSn(OH)_6$, $SrSn(OH)_6$, and ZnO. We also found out that there is a linear correlativity between the truncated degrees and the amount of NaOH when studying morphological evolution behavior from an octahedron to a cube of ZTO.

Introduction

Chemical synthesis of morphology-controlled single crystals on the microscale and nanoscale has received extensive scientific and technological attention because of these crystals' peculiar physical and chemical properties related to different crystal facets.[1−5] A number of polyhedral-shaped crystals, such as oxides and noble metals, have been reported. However, nearly all of these shape-controlled synthetic examples were realized by means of introducing certain adscititious influences into their reaction systems, such as surfactants, inorganic anions, or physical or chemical stimulation.[1,4−18] These factors are proposed to alter the order of surface free energies of different facets or to change the relative growth rates along different orientations in a solution phase.[6] Despite the successes, most of these processes depended on an appropriate choice of effective interactions between the surfactants or anions and the target compounds. As a result, these examples are usually limited to some specific systems.

Crystal habits result from the difference in growth rates along different crystallographic faces, so an essential way to investigate the complex processes is by analyzing the mechanism thermodynamically and dynamically. It is known that both the intrinsic crystal structures and physical or chemical conditions serve as important factors that govern the equilibrium shapes of crystals, as crystals of each crystal system have a tendency to exhibit certain definite simple shapes or their combination forms, and in the meantime, the morphologies can also be modified by some external disturbance. Many structures of different dimensions and shapes have been achieved experimentally. However, crystallization is still a process far from being well understood, because crystal growth is a complex process involving the arrangement of millions of atoms or molecules near the surface area, and it is further complicated by the interactions between atoms and influences from the surroundings. Several theoretical growth models have been proposed to accomplish an in-depth

*To whom correspondence should be addressed. E-mail: wangxun@mail.tsinghua.edu.cn.

(1) Tian, N.; Zhou, Z. Y.; Sun, S. G.; Ding, Y.; Wang, Z. L. *Science* **2007**, *316*, 732–735.
(2) Hu, L. H.; P., Q.; Li, Y. D. *J. Am. Chem. Soc.* **2008**, *130*, 16136–16137.
(3) Tao, A.; Sinsermsuksakul, P.; Yang, P. D. *Angew. Chem., Int. Ed.* **2006**, *45*, 4597–4601.
(4) Wu, B. H.; G., C.; Zheng, N. F.; Xie, Z. X.; Stucky, G. D. *J. Am. Chem. Soc.* **2008**, *130*, 17563–17567.
(5) Zhou, K. B.; Wang, X.; Sun, X. M.; Peng, Q.; Li, Y. D. *J. Catal.* **2005**, *229*, 206–212.
(6) Wang, Z. L. *J. Phys. Chem. B* **2000**, *104*, 1153–1175.
(7) Ma, Y. Y.; Kuang, Q.; Jiang, Z. Y.; Xie, Z. X.; Huang, R. B.; Zheng, L. S. *Angew. Chem., Int. Ed.* **2008**, *47*, 8901–8904.
(8) Geng, B. Y.; Fang, C. H.; Zhan, F. M.; Yu, N. *Small* **2008**, *4*, 1337–1343.
(9) Wiley, B.; Sun, Y. G.; Chen, J. Y.; Cang, H.; Li, Z. Y.; Li, X. D.; Xia, Y. N. *MRS Bull.* **2005**, *30*, 356–361.
(10) Sun, Y. G.; Xia, Y. N. *Science* **2002**, *298*, 2176–2179.
(11) Ahmadi, T. S.; Wang, Z. L.; Green, T. C.; Henglein, A.; El Sayed, M. A. *Science* **1996**, *272*, 1924–1926.
(12) Seo, D.; Park, J. C.; Song, H. *J. Am. Chem. Soc.* **2006**, *128*, 14863–14870.
(13) Kim, F.; Connor, S.; Song, H.; Kuykendall, T.; Yang, P. D. *Angew. Chem., Int. Ed.* **2004**, *43*, 3673–3677.
(14) Pietrobon, B.; Kitaev, V. *Chem. Mater.* **2008**, *20*, 5186–5190.
(15) Lee, H.; Habas, S. E.; Kweskin, S.; Butcher, D.; Somorjai, G. A.; Yang, P. D. *Angew. Chem., Int. Ed.* **2006**, *45*, 7824–7828.
(16) Li, C. C.; Shuford, K. L.; Park, Q. H.; Cai, W. P.; Li, Y.; Lee, E. J.; Cho, S. O. *Angew. Chem., Int. Ed.* **2007**, *46*, 3264–3268.
(17) Seo, D.; Yoo, C. I.; Park, J. C.; Park, S. M.; Ryu, S.; Song, H. *Angew. Chem., Int. Ed.* **2008**, *47*, 763–767.
(18) Yang, H. G.; Sun, C. H.; Qiao, S. Z.; Zou, J.; Liu, G.; Smith, S. C.; Cheng, H. M.; Lu, G. Q. *Nature* **2008**, *453*, 638–642.

Published on Web 09/25/2009

Scheme 1. Elementary Processes of Surface Construction Based on Kossel's Model

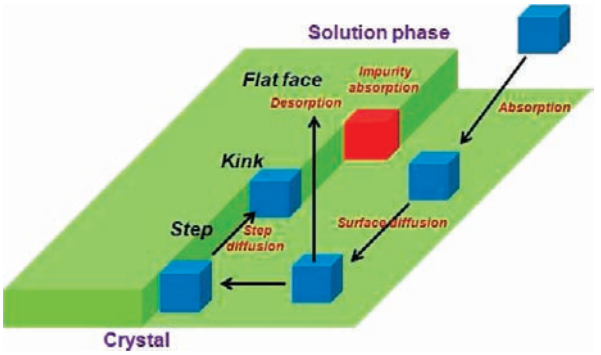

understanding of such assembly behaviors, including Bravais–Friedel–Donnay–Harker law,[19–21] Kossel's model,[22,23] the Burton–Cabrera–Frank model,[24,25] periodic bond chain (PBC) theory,[26] and the anion coordination polyhedron growth unit theory mode.[27]

These interface models were based on a rational structural hypothesis of the growing crystal surfaces, and reactions on surfaces were considered as the key steps in the whole growth process. A well-accepted interface growth theory is Kossel's model, which suggests that a flat growing crystal surface is actually made of moving layers of monatomic height, known as steps, containing a certain number of kink sites.[22,28] Growth units are most easily incorporated into a crystal body at kinks because of the abundance of unsaturated lateral bonds, and this is also consistent with the growth mode of the K face mechanism in PBC theory of Hartman and Perdok.[26] Therefore, it is reasonable that there is still a surface diffusion process during the time from the adsorption of growth units on the crystal surface to their incorporation into the crystal body at active sites. And, the diffusion process is actually a kind of reconstruction process of the surface structures. A typical construction process of a growing surface is illustrated in Scheme 1, which depicts the fundamental actions of a growth unit on a surface. It is well-known that crystal habits can be effectively modified by introducing appropriate additives. The phenomena can also reasonably be interpreted in terms of their competitive absorption onto the active sites. A growth mode would be altered when the coordination structures of impurity units with kinks are more stable than those of growth units.[28] Hence, the stability is determined by the structures of ligands and crystals as well as their surface interactions, so the diversity of coordination structures may also account for the limitation of an additive-adopted specific synthesis.

Surface reconstruction by means of atomic diffusion is a time-consuming dynamic process, so it would be feasible to get crystals with simple or combination shapes by controlling their well-grown surfaces. We have discovered that the shape-controlled synthesis of nanocrystals can be achieved via pretreating the precursors. Herein, we employ zinc tin oxide (Zn_2SnO_4; ZTO) as a model compound to illustrate an effective method to realize the shape-selected synthesis of nanocrystals based on the surface reconstruction of growing nuclei. ZTO octahedral crystals were prepared in the absence of any additives, and the aqueous solution reaction system merely consisted of $SnCl_4$, $Zn(CH_3COO)_2$, and NaOH. The whole synthetic procedure include two steps: pretreating reactant mixture by stirring at room temperature and a succedent hydrothermal treatment in a Teflon autoclave at 200 °C. To further verify the general applicability of this idea, we also successfully applied the method to the controlled synthesis of $CaSn(OH)_6$, $SrSn(OH)_6$, and ZnO as more evidential complementarities.

Experimental Section

Chemicals. All of the reagents used in this work were purchased from the Beijing Chemical Reagent Company, including sodium hydroxide (NaOH), zinc acetate hexahydrate ($Zn(CH_3COO)_2\cdot 6H_2O$), tin chloride pentahydrate ($SnCl_4\cdot 5H_2O$), calcium nitrate tetrahydrate ($Ca(NO_3)_2\cdot 4H_2O$), and strontium acetate hemihydrate ($Sr(CH_3COO)_2\cdot 0.5H_2O$). They were of analytical grade and used without any treatment. Deionized water was the only solvent.

Preparation of ZTO Octahedral Crystals. In a typical synthetic procedure, 8 mmol of NaOH, 0.25 mmol of $SnCl_4$, and 0.5 mmol $Zn(CH_3COO)_2$ were added successively into a 40 mL Teflon-lined autoclave with 30 mL of deionized water under magnetic stirring at room temperature (around 25 °C). After 2 h of subsequent stirring, the reaction system was sealed and kept at 200 °C for 5 days. Thus, octahedral ZTO single crystals would be obtained. By reducing the reaction time, polycrystalline precursors at different stages can be separated. The products were separated by centrifugation and washed with ethanol three times.

By reducing the amount of NaOH, such as 2 mmol, truncated octahedral ZTO crystals can be prepared. Aggregation of ZTO particles was obtained similarly without 2 h of stirring. Samples of the precursors for TEM characterization were prepared directly at room temperature after 2 h of stirring or direct mixing.

Preparation of $CaSn(OH)_6$, $SrSn(OH)_6$, and ZnO Crystals. In a typical synthetic procedure, 4 mmol of NaOH, 0.25 mmol of $SnCl_4$, and 0.5 mmol of M (M = $Ca(NO_3)_2$, $Sr(CH_3COO)_2$) were added successively into a 40 mL Teflon-lined autoclave with 30 mL of deionized water under magnetic stirring at room temperature (around 25 °C); for the synthesis of ZnO nanorods, the raw materials were composed of 8 mmol NaOH and 0.5 mmol $Zn(CH_3COO)_2$. After two-hour subsequent stirring, the reaction system was sealed and kept at 200 °C for 24 h. The products were also separated by centrifugation and washed with ethanol for several times. Contrastive synthesis was conducted in a similar way merely without 2 h of stirring at room temperature.

Characterization. The size and morphology of these compounds were determined by JEOL JEM-1200EX transmission electron microscope (TEM) at 100 kV, using a Tecnai TF20 S-Twin high-resolution transmission electron microscope (HRTEM) at 200 kV and a JEOL JSM-6700F scanning electron microscope (SEM). Samples were prepared by dropping dilute ethanol dispersion of the products onto the surface of a carbon coated copper grid and silicon wafer for TEM and SEM, respectively. The phase purity of the products was examined by XRD on a Bruker D8 Advance X-ray diffractometer using Cu Kα radiation (λ = 1.5418 Å).

(19) Bravais, A. *Études Cristallographic*; Gauthier-Villars: Paris, 1866.
(20) Friedel, M. G. *Bull. Soc. Fr. Mineral. Cristallogr.* **1907**, *30*, 326–455.
(21) Donnay, J. D. H.; Harker, D. *Am. Mineral.* **1937**, *22*, 446–467.
(22) Kossel, W; Nachr, G.; Wiss, G. *Math-Phys. Kl.* **1927**, 135–143.
(23) Stranski, I. N. *Z. Phys. Chem.* **1928**, *136*, 259–278.
(24) Burton, W. K.; Cabrera, N.; Frank, F. C *Nature* **1949**, *163*, 398–399.
(25) Burton, W. K.; Cabrera, N.; Frank, F. C. *Phil. Trans. R. Soc., London* **1951**, *243*, 299–358.
(26) Hartman, P.; Perdok, W. G. *Acta Crystallogr.* **1955**, *8*, 49–52.
(27) Li, W. J.; Shi, E. W.; Zhong, W. Z.; Yin, Z. W. *J. Synth. Cryst.* **1999**, *28*, 117–125.
(28) Mutaftschiev, B. *The Atomistic Nature of Crystal Growth*, 1st ed.; Springer-Verlag: Berlin, 2001.

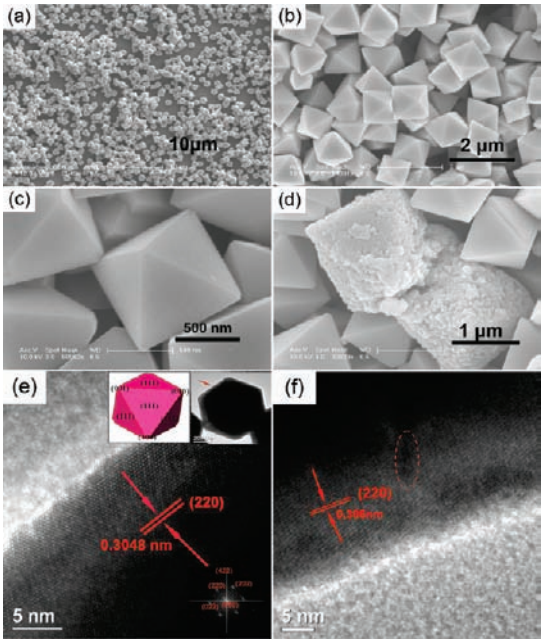

Figure 1. ZTO single crystals synthesized at 200 °C for 5 days. (a) Overall SEM image of octahedral ZTO single crystals. (b, c) SEM images under different magnifications. (d) Early octahedra in single-crystal products. (e) HRTEM analysis near surface area. Insets (top right and top left) indicate the area selected for HRTEM analysis and the corresponding geometrical analogy; the inset (bottom) is the Fourier transformation result of the HRTEM image. (f) Residual grain boundary in ZTO single crystals marked with a dashed line.

Results and Discussion

Single Crystals, Intermediates, and Precursors of Octahedral ZTO. Figure 1a−c show SEM images of typical Zn_2SnO_4 octahedral single crystals synthesized at 200 °C for 5 days. The overall images under low magnification indicate a high purity yield and smooth surfaces, while the magnified image (Figure 1c) reveals that the corners of these octahedra are slightly truncated. To determine the single-crystal character and their exposed facets, these octahedral crystals were analyzed by HRTEM near the surface areas, as shown in Figure 1e and f (see also, Figure S1 in the Supporting Information). It is obvious that their surfaces are enclosed by {111} facets, as illustrated in Figure 1e (the inset on top-left is analogous to the TEM image in the top-right one). Calculated from the lattice fringes of HRTEM images, the lattice spacing is about 0.3048 nm, and it corresponds to the (220) facet of ZTO. According to the Fourier transformation of the HRTEM image (shown as the bottom inset), the direction vector **B** of the incident electron beams is determined to be $[\bar{1}11]$, which further conforms the exposing {111} facets. There are still a few residual grain boundaries on the surfaces of some crystals, as shown by the dashed line in Figure 1f, which provides evidence for our conclusion that these single crystals were evolved from their polycrystalline forms. Further characterizations were used to learn their phase and composition. The powder X-ray diffraction pattern (see Figure 4a) can be well indexed to face-centered cubic (fcc) Zn_2SnO_4 (JCPDS 74−2184). And, the energy dispersive X-ray spectrum (EDS) analysis (see Figure 4e) of ZTO single crystals confirms that the products consist only of Zn, Sn, and O without any other mixed elements.

Accordingly, it is clear that octahedral ZTO single crystals enclosed by {111} facets can be synthesized successfully merely via pretreating the precursors by stirring. The results show an approach to realizing crystal growth on the basis of the crystal self-limitation property. To clarify the growth process, we further investigated the growth mechanism in detail by preparing intermediates for different reaction times.

Figure 2a,b and Figure S2 (Supporting Information) are SEM images of the intermediate ZTO crystals prepared by decreasing the reaction time from 5 days to 24 h. The products also display a large quantity and a good uniformity in size. It can be observed that there are many particles attached on the surfaces of these polyhedral crystals from Figure 2b and Figure S2b (Supporting Information). And, many noncompact and broken octahedral crystals also exist there (see Figure 2c and also Figure S2). The results indicate that they are not perfect octahedral single crystals, and accordingly we speculate that they were formed through three-dimensional aggregates of tiny particles formed by the precipitation of reactants. Further analysis by HRTEM was employed to validate this conclusion. It can be clearly observed from Figure 2e,f and Figure S3 (Supporting Information) that their surface areas are composed of tiny grains with random misorientations, which confirms the polycrystalline character of those intermediates. The peaks of the XRD pattern (Figure 4b) also match well with the literature result (JCPDS 74-2184). Figure 2d shows a SEM image of the product after 10 h of hydrothermal reaction. They are octahedra with holes and particles on the surfaces, showing that the phase and octahedral shapes of these ZTO crystals formed during the process of hydrothermal treatment. So it is safe to conclude that the octahedral ZTO single crystals evolve from their corresponding octahedral polycrystals which are formed via the assembly of disordered nanoparticles. The conclusion can be further proved by the detection of some incomplete octahedral polycrystals in those single-crystal products, as shown in Figure 1d.

It has been found experimentally that the formation of ZTO octahedral crystals strongly depends on an appropriate pretreatment of the precursors at room temperature. In the procedure, 2 h of stirring is essential to their formation. Though the major products are aggregated nanoparticles, there have been many polyhedral precursors after 2 h of stirring, as shown in Figure 3a (see also Figure S4 in the Supporting Information), which suggests that those tiny particles after pretreatment have a tendency to assemble into polyhedral crystals. Their phase mainly belongs to $Zn(OH)_2$, according to the XRD pattern (see Figure 4c, JCDPS 38-0385). It is interesting that the shape of these polyhedra exhibits a symmetry type of 222, and it is consistent with the space group $P2_12_12_1$ of $Zn(OH)_2$. In contrast, direct hydrothermal treatment for 24 h without sufficient stirring just resulted in some random aggregations of ZTO nanoparticles with a size of ~5 nm (see Figure 3b,c). The precursors without stirring are a disordered aggregation of tiny particles (Figure 3d), and the phase can also be indexed to $Zn(OH)_2$ (see Figure 4d, JCDPS 38-0385). Observed from the HRTEM result shown in Figure 3e,f, the crystallization of these early seeds by direct mixing is poorer than those after pretreatment.

Consequently, pretreating the precursors at an early stage affected the later crystal growth process occurring

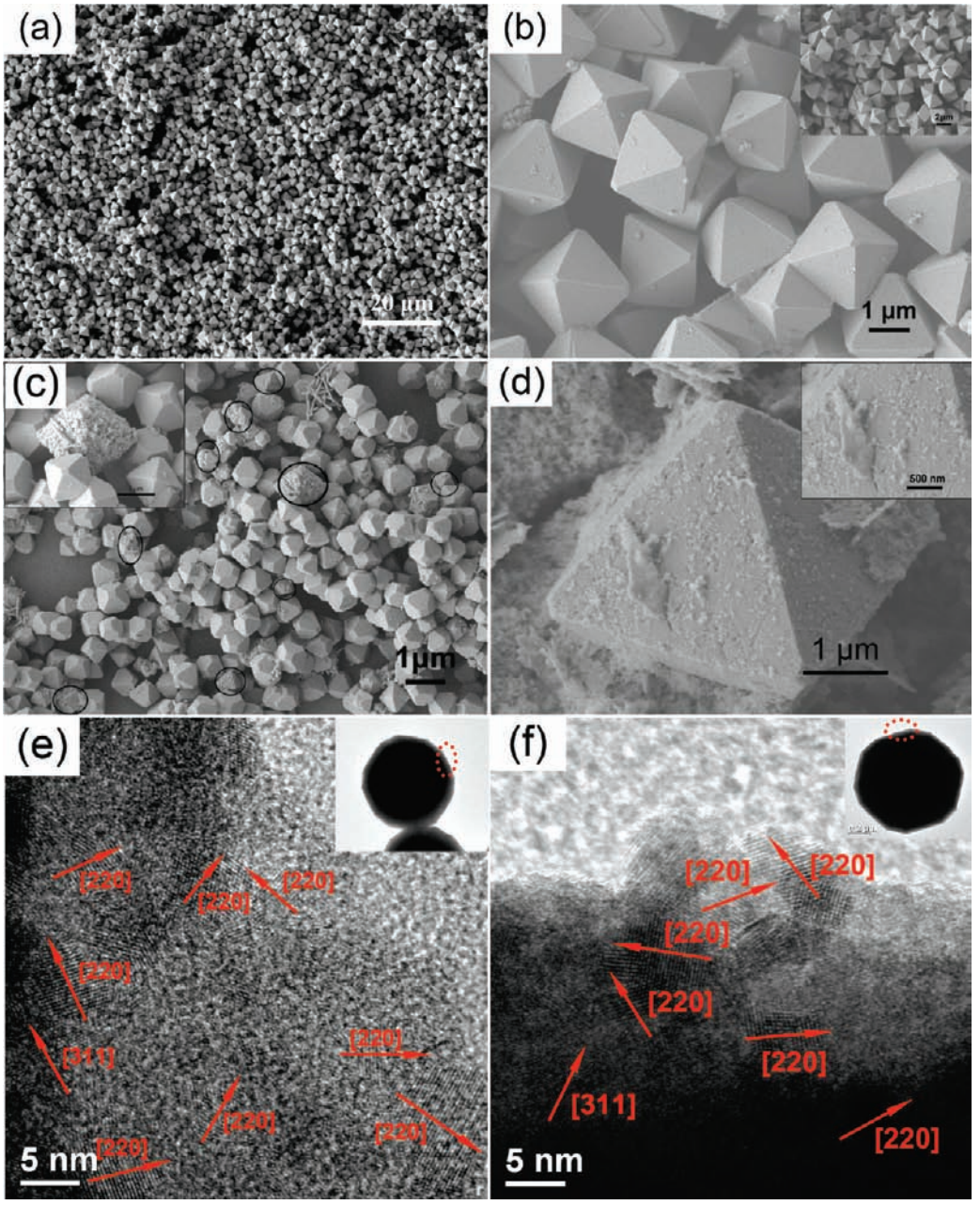

Figure 2. Polycrystals of ZTO synthesized at 200 °C by decreasing the reaction time to 24 h. (a) SEM image under low magnification. (b) SEM image under high magnification. The inset is the selected area. (c) SEM images showing some incompact and broken octahedral crystals. (d) SEM image of an intermediate octahedron after 10 h of reaction. (e, f) HRTEM analysis of the surface areas, which are composed of tiny grains with random misorientation. The insets are corresponding sites selected for analysis.

under hydrothermal conditions. Though they are the same reaction system, a difference in the states of their precursors at room temperature caused by stirring can be reflected in subsequent growth behaviors. Therefore, we can deduce that some important processes have occurred on the surfaces of these nuclei during the 2 h, and they can have a critical influence on later growth.

Truncated Octahedral ZTO Crystals. Similarly, truncated octahedral ZTO crystals could be fabricated just by reducing the amount of NaOH, and the truncated degree of corners varies with the amount of NaOH. Figure 5a shows a typicial SEM image of these truncated octahedral ZTO crystals prepared by reducing the amount of NaOH to 2 mmol. The XRD pattern also matches Zn_2SnO_4 (Figure 4f). In addition to the morphology of the final products, states of the precursors after pretreatment and their phases also undergo some changes. It is clear that there is a large percentage of cubes in the aggregation of nanoparticles displayed in Figure 5b. And, the XRD pattern (Figure 4h) can be indexed to $ZnSn(OH)_6$ (JCDPS 20-1455) rather than $Zn(OH)_2$, which can be attributed to amphoteric property of zinc and tin hydroxides. In the pretreatment process, nanoparticles partly assembled into a cube shape, a kind of simple shape of $ZnSn(OH)_6$ of the fcc structure. Results by direct hydrothermal reaction without pretreatment are still aggregated nanoparticles (Figure 5c) of Zn_2SnO_4 according to the XRD result in Figure 4g. And, the precursors are

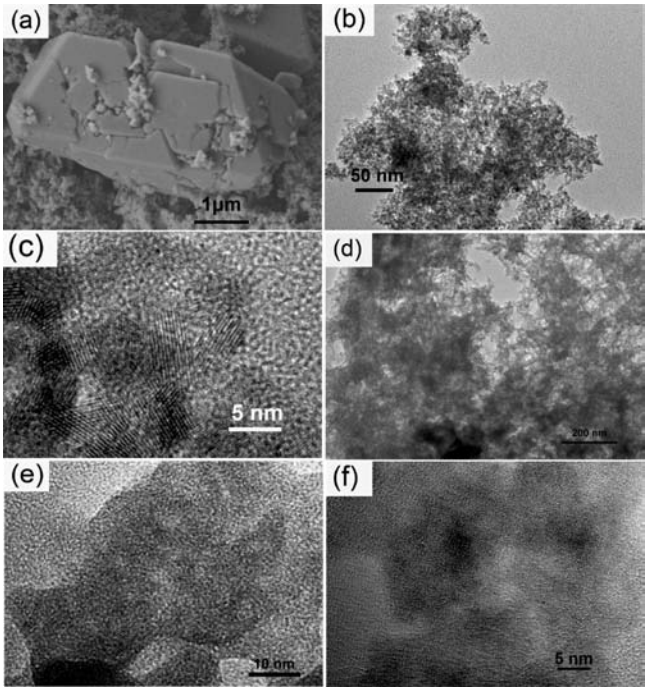

Figure 3. (a) SEM image of the precursor after 2 h of stirring. (b, c) TEM and HRTEM images of resultants by direct hydrothermal treatment without sufficient stirring. (d) TEM image of the precursor by direct mixing of reactants without sufficient stirring. (e) HRTEM image of the precursor after 2 h of stirring. (f) HRTEM images of the precursor by direct mixing of reactants without sufficient stirring.

also random aggregations of $ZnSn(OH)_6$ nanoparticles (see Figure 5d and Figure 4i). Though the initial precursors of octahedra and truncated octahedra are $Zn(OH)_2$ and $ZnSn(OH)_6$, respectively, they share a similar growth route, so it may imply that the strategy is effective in both systems.

Mechanism Analysis. As mentioned above, the whole processes contain two steps. Because of the amphoteric properties of zinc and tin hydroxides, the concentration of sodium hydroxide will have an obvious influence on the results of the precursors. Phase transformation processes can be illustrated by the following equations:

$$Sn^{4+} + OH^-(8\ mmol) \xrightarrow{rt} Sn(OH)_6^{2-}$$

$$Zn^{2+} + OH^-(8\ mmol) \xrightarrow{rt} Zn(OH)_2 + Zn(OH)_4^{2-}$$

$$Sn(OH)_6^{2-} + Zn(OH)_2 \xrightarrow{200\ °C} Zn_2SnO_4 + H_2O + OH^- \quad (1)$$

$$Sn^{4+} + Zn^{2+} + OH^-(2\ mmol) \xrightarrow{rt} ZnSn(OH)_6 + Zn(OH)_4^{2-}$$

$$ZnSn(OH)_6 + Zn(OH)_4^{2-} \xrightarrow{200\ °C} Zn_2SnO_4 + H_2O + OH^- \quad (2)$$

Though differences exist in both morphologies and phases of the precursors after 2 h of pretreatment by stirring, they still follow the same formation route. From the results above, we can see that these nanoparticles after pretreatment have a tendency to assemble together, which is different from the results by direct mixing. Their crystal structures and surface states might have developed during the 2 h, and the ability further enables these disordered nanoparticles to assemble into a polyhedral shape at room temperature or under high-temperature conditions. On the basis of the growth route using Kossel's model, we propose that this ability originates from the surface reconstruction by means of surface diffusion. From the structural comparison of the precursory particles pretreated and untreated in Figure 3e,f, we can see that those particles after pretreatment have exhibited a developed crystal character, while untreated precursors are gels with quite poor crystallization. These embryonal facets will allow these nanoparticles to attach together and form an obvious simple shape both at room temperature and at high temperatures, as the results shown in Figures 2c and 3a. Because the formation of crystal facets takes place over a certain time, sufficient time for surface reconstruction of the nuclei at the early stages is important for realizing self-limitation-based growth to display a polyhedral shape.

Investigation of a detailed growth mechanism of these ZTO crystals remains a challenge; in spite of this, some clues and proposed models can be helpful. In the absence of any surfactants, surfaces of these precursory particles can only be capped with adsorptive hydroxyl groups (−OH) and water molecules. It has been suggested that the condensation reactions between nonbridging hydroxyl groups would lead to hard agglomerates of nanoparticles because of the formation of oxide bridges.[29,30] The reaction can be simplified as $M-OH + HO-M \rightarrow M-O-M + H_2O$. This is actually a universal and fundamental process in hydrolysis, agglomerate, and sol−gel reactions. In our system, hydroxyl condensation reactions undoubtedly serve as a bonding force for the assembly of nanoparticles into polyhedral shapes of $Zn(OH)_2$ and Zn_2SnO_4. And, the mass transfer processes can be enhanced by stirring and the hydrothermal reaction at 200 °C by providing a driving force for their motion.

Comparing the results at different times, it is noted that there is a decrease in the size of these polyhedral crystals from the polycrystal intermediates to the final single crystals (see Figures 1b and 2b,d). Because the octahedral intermediates are incompact polycrystals with many nanoparticles attaching on their surfaces, as displayed in Figure 2 and Figure S2 (Supporting Information), they are not thermodynamically stable because of the high surface energy. There is a further coarsening process of the particles after their assembly, resulting in smooth surfaces (see Figure 1e,f and Figure S1, Supporting Information). As the particles have not been confined to the crystal bodies before the formation of chemical bonds, it is easy for them to disassemble from the surfaces to form new crystals or to attach onto other octahedra, leading to a decrease in size.

(29) Paulaime, A. M.; Seyssiecq, I.; Veesler, S. *Powder Technol.* **2003**, *130*, 345–351.
(30) Jones, S. L. N. *J. Am. Ceram. Soc.* **1988**, *71*, C-190–1.

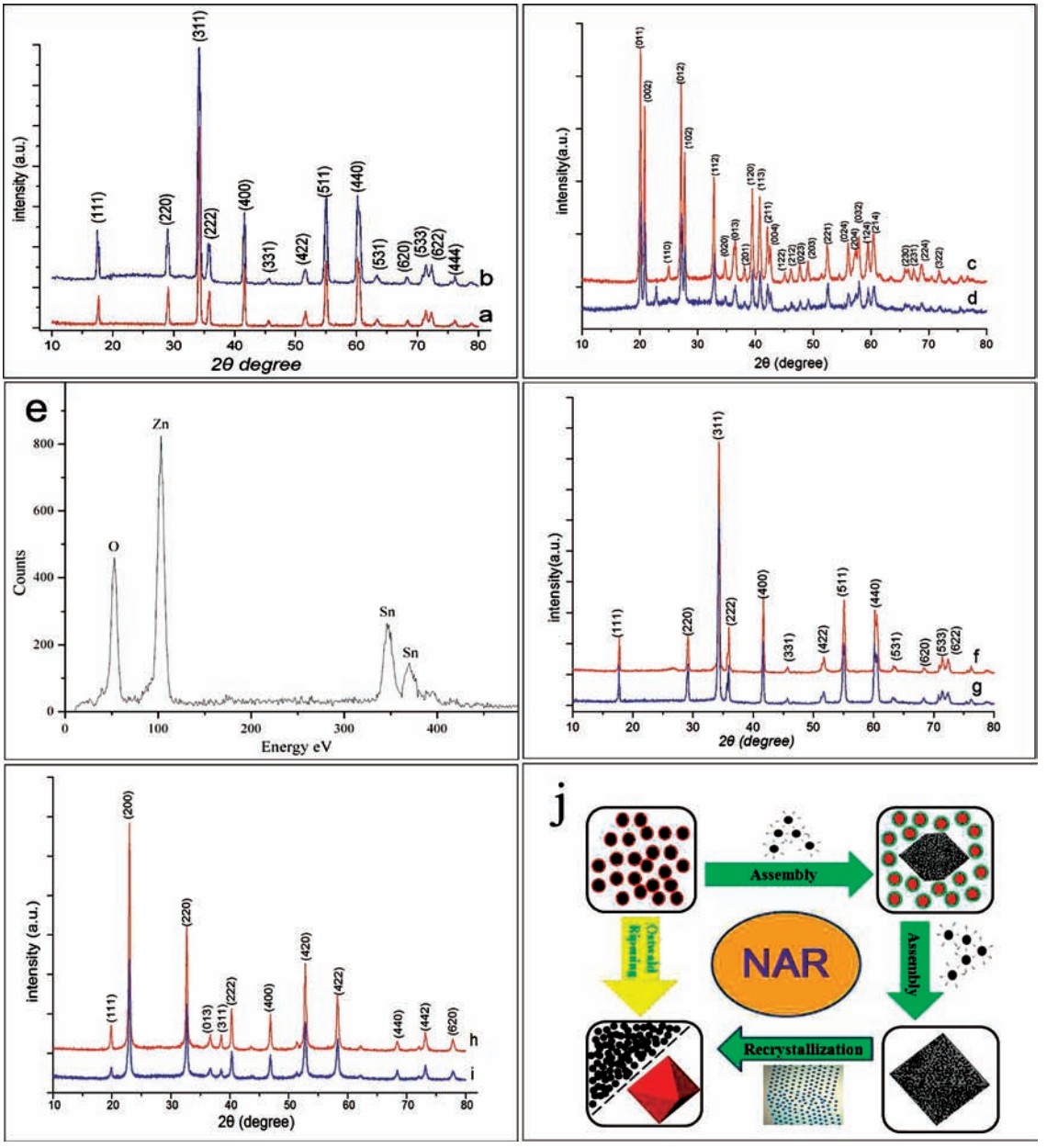

Figure 4. (a, b) XRD patterns of octahedral single crystals and polycrystals. (c, d) XRD patterns of precursors after 2 h of stirring at room temperature and precursors prepared by direct mixing corresponding to a and b. (e) EDS analysis of ZTO single crystal. (f, g) XRD patterns of truncated ZTO octahedra and aggregation products after hydrothermal treatment without stirring. (h, i) XRD patterns of precursors after 2 h of stirring at room temperature and precursors prepared by direct mixing corresponding to f and g. (j) Scheme of the nucleation−assembly−recrystallization (NAR) mechanism.

In solution systems, the process is usually interpreted in terms of Ostwald ripening. Research on polycrystals and oriented attachment processes has also revealed that direct atom diffusion across grain boundaries and an orientation change of the particles via grain rotation will result in deformation and phase transformation.[31−36] The two basic forms of mass transfer in a crystallization process can be termed the solvent-mediated dissolution−crystallization mechanism and the grain boundary-mediated in situ transformation mechanism. It would be reasonable to say that both ways exist in the recrystallization process of octahedral ZTO from polycrystals to single crystals. In the process of recrystallization, surface and unassembled particles exposed to the solvent might undergo dissolution to a certain extent and lead to smooth facets with fewer adsorptive particles, especially at keen-edged parts with a relatively higher surface energy. Meanwhile, those inner particles, which are surrounded reciprocally and relatively free from water, primarily follow the in situ transformation mechanism, which is proved by the residual grain boundary in Figure 1f. Atoms on boundaries will diffuse from one

(31) Margulies, L.; Winther, G.; Poulsen, H. F. *Science* **2001**, *291*, 2392–2394.
(32) Shan, Z. W.; Stach, E. A.; Wiezorek, J. M. K.; Knapp, J. A.; Follstaedt, D. M.; Mao, S. X. *Science* **2004**, *305*, 654–657.
(33) Pusey, P. N. *Science* **2005**, *309*, 1198–1199.
(34) Lipowsky, P.; Bowick, M. J.; Meinke, J. H.; Nelson, D. R.; Bausch, A. R. *Nat. Mater.* **2005**, *4*, 407–411.
(35) Banfield, J. F.; Welch, S. A.; Zhang, H. Z.; Ebert, T. T.; Penn, R. L. *Science* **2000**, *289*, 751–754.
(36) Pacholski, C.; Kornowski, A.; Weller, H. *Angew. Chem., Int. Ed.* **2002**, *41*, 1188–1191.

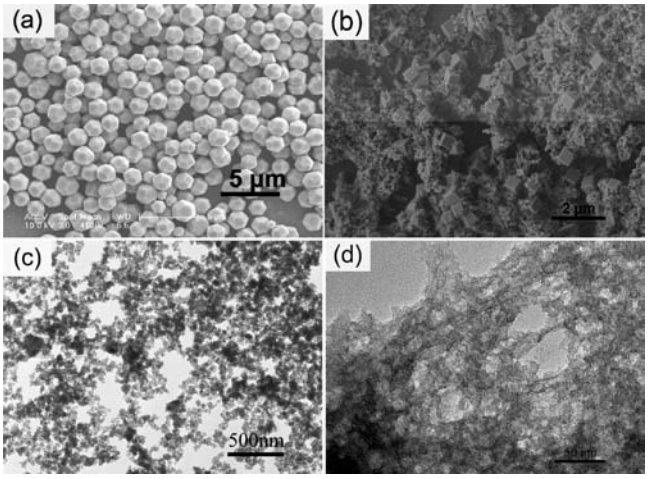

Figure 5. (a) SEM image of truncated octahedral ZTO crystals prepared by reducing the amount of NaOH to 2 mmol. (b) SEM image of precursors after 2 h of stirring at room temperature. (c) TEM image of ZTO aggregation prepared by reducing the amount of NaOH to 2 mmol without stirring. (d) TEM image of the precursors corresponding to (c).

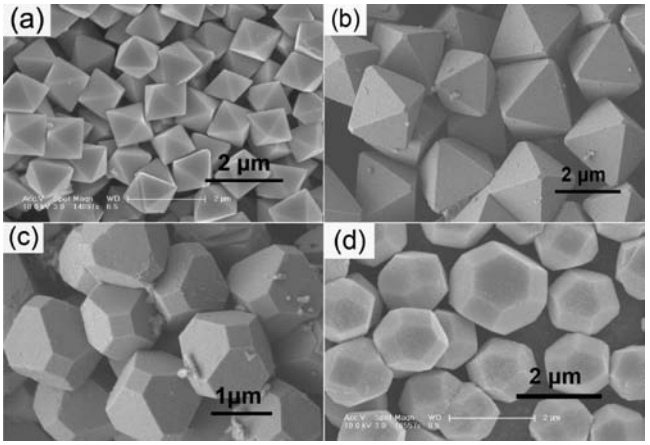

Figure 6. SEM images of evolutive morphologies of ZTO octahedral crystals by employing different amounts of sodium hydroxide: (a) 8 mmol, (b) 6 mmol, (c) 4 mmol, and (d) 2 mmol.

Table 1. t Values of the Morphologies in Figure 6

	a	b	c	d
n_{NaOH}/mmol	8	6	4	2
t	1.73	1.64	1.37	1.10

grain to another, resulting in migration of the grain boundary and crystal growth.

From the discussed proposal of the ZTO formation process from the room temperature stage to the high-temperature reaction, the whole growth mechanism can be expressed by two basic processes after nucleation: assembly and recrystallization. We refer to the whole strategy as a nucleation−assembly−recrystallization (NAR) mechanism, as illustrated in Figure 4j. Assembly denotes the formation of octahedral polycrystalline structures through sufficient pretreatment at room temperature and an early hydrothermal treatment based on surface reconstruction. Recrystallization describes the transformation of ZTO octahedra from polycrystals to single crystals under hydrothermal conditions.

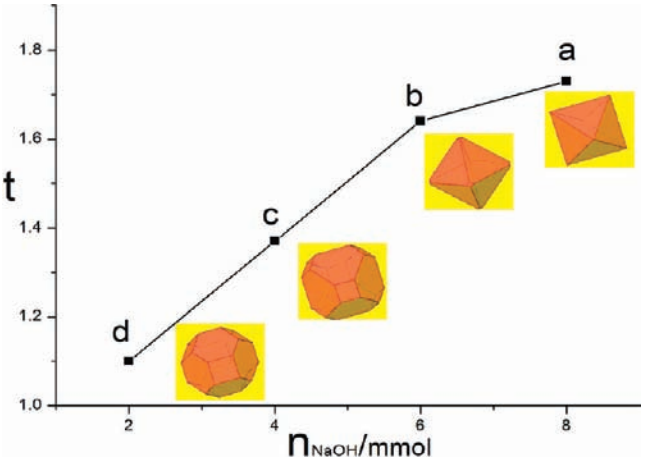

Figure 7. The correlativity of truncated degree with the amount of NaOH.

Morphological Evolution of ZTO Octahedra with the Amount of Sodium Hydroxide. The discussed results have also shown that the morphologies of ZTO crystals can evolve from an octahedron to a truncated octahedron when reducing the amount of sodium hydroxide, in spite of the differences in phases and shapes of the intermediates. In order to get an in-depth understanding of this trend, we further studied the morphological evolution behavior by adjusting the ratio of NaOH to tin and zinc salts. Figure 6 displays the evolution process from an octahedron to a truncated octahedron. The truncated degree varies obviously with the amount of NaOH, while the amounts of $SnCl_4$ and $Zn(CH_3COO)_2$ keep constant at 0.25 mmol and 0.5 mmol, respectively.

In order to evaluate the truncated degree using a quantitative standard, we introduce a parameter t to denote different evolutions between an octahedron and a cube, which share a symmetry type of O_h. Because the combinations of an octahedron and a cube are covered with six {100} facets and eight {111} facets, we define a shape-relating function in the form of $t = d_{100}/d$ to describe the evolution from an octahedron to a cube, where d_{100} is the distance from the center to the {100} facets and d_{111} is the distance from the center to the {111} facets. Obviously, the value of t ranges from $\sqrt{3}/3$ to $\sqrt{3}$; $\sqrt{3}$ denotes an octahedron and $\sqrt{3}/3$ corresponds to a perfect cube. Additionally, the open interval ($\sqrt{3}/3$, $\sqrt{3}$) describes combinational forms with different truncated degrees.

With the aid of Shape V7, a program to calculate and display the morphology and symmetry of single crystals, we are able to simulate these combinational shapes and get their parameters t from distances given by the program. The t values are listed in the Table 1, according to the simulation of these morphologies in Figure 6.

Figure 7 shows the correlativity of t and the amount of NaOH, and the insets are their corresponding simulations. The result indicates that there is a linear correlativity between the truncated degrees and the amount of NaOH. In the interval of a and b, there might exist an inflection to terminate the linear relationship, at which the lowest amount of NaOH to obtain a complete octahedron can be seen .

More Applications of This Idea. Thus, we have shown an effective approach to controlling the morphologies of

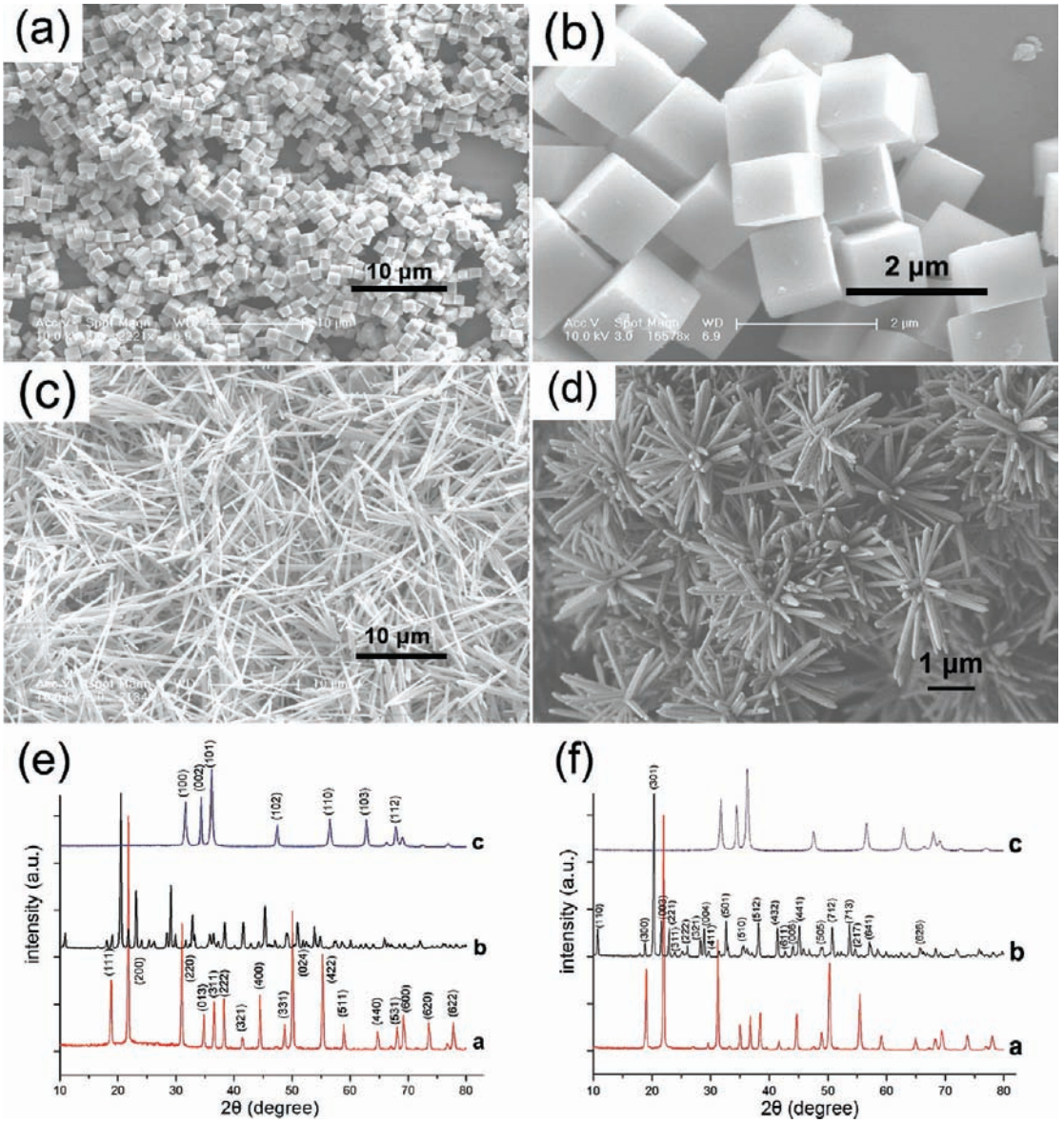

Figure 8. SEM images of other compounds after 2 h of pretreatment: (a, b) $CaSn(OH)_6$, (c) $SrSn(OH)_6$, (d) and ZnO. (e) XRD patterns of these compounds after 2 h of stirring. (f) XRD patterns of these compounds without 2 h of stirring (a, $CaSn(OH)_6$; b, $SrSn(OH)_6$; c, ZnO).

ZTO crystals from an octahedron to a cube by pretreating precursors at room temperature. The basic principle lies in sufficient surface reconstruction after nucleation. To further verify this idea, we applied it to $CaSn(OH)_6$, $SrSn(OH)_6$, and ZnO. Figure 8a−d are the SEM images of these compounds, prepared by stirring their precursors for 2 h at room temperature and a succedent reaction at 200 °C for 24 h. The products, cubes of $CaSn(OH)_6$, nanowires of $SrSn(OH)_6$, and nanorods of ZnO, also exhibit large quantity yields and good uniformity in size. Their phases were determined by XRD results, as shown in Figure 8e ($CaSn(OH)_6$, JCPDS 74-1823; $SrSn(OH)_6$, JCPDS 09-0086; ZnO, JCPDS 36−1451). The difference in morphologies can be ascribed to their difference in crystal structures. Crystals of cubic systems usually display a cube or octahedron shape, such as Zn_2SnO_4 and $CaSn(OH)_6$, whereas $SrSn(OH)_6$ and ZnO, crystals of a hexagonal system, have a tendency to grow along the *c* axis to form a one-dimentional structure, such as rods and wires.

To further test the influence of surface reconstruction on the results of crystal growth, we also prepared these compounds by direct hydrothermal treatment without pretreating the precursors. Figure 8f shows the XRD results of these contrastive examples, which are consistent with the patterns in Figure 8e. The results characterized by SEM are shown in Figure 9. It is apparent that their fine structures have changed compared with the results in Figure 8. A low-magnification SEM image (Figure 9a) also presents many cubes of $CaSn(OH)_6$, but their uneven surface structures are quite different from those smooth cubes in Figure 8b. The contrastive results offer more rational evidence of the influence of sufficient surface diffusion at early stages on the growth behaviors of inorganic crystals. Additionally, even apparent morphological changes of $SrSn(OH)_6$ and ZnO (Figure 9c,d) provide further exemplifications for this mechanism.

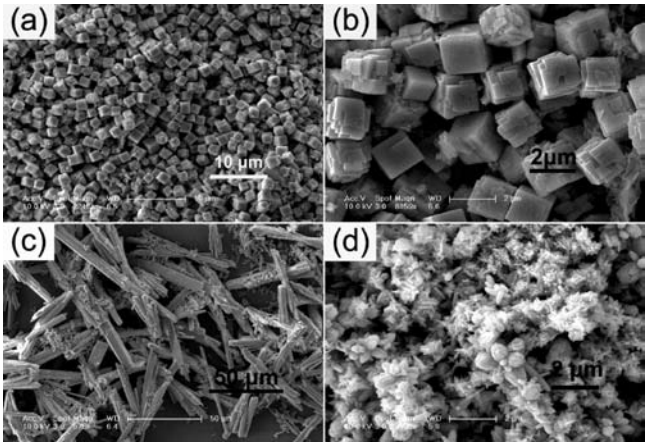

Figure 9. SEM images of other compounds without 2 h of pretreatment: (a, b) $CaSn(OH)_6$, (c) $SrSn(OH)_6$, and (d) ZnO.

Conclusions

In conclusion, on the basis of a simple idea of a surface reconstruction process of nuclei by means of surface diffusion, we have displayed an effective method to carry out shape-selected growth of ZTO octahedral and truncated octahedral structures. These crystals were formed via the assembly of precursory nanoparticles and a recrystallization process after nucleation in the absence of any additives. Different states of precursors at room temperature can affect the subsequent crystal growth behaviors, leading to different evolutive results. The method can also be applied to the synthesis of $CaSn(OH)_6$ cubes, $SrSn(OH)_6$ nanowires, and ZnO nanorods. In these examples, the shape-selected growth of nanocrystals was influenced by surface processes. And, the morphology evolution behavior from an octahedron to a cube of ZTO exhibits a linear correlativity between the truncated degrees and the amount of NaOH. The NAR mechanism displays an approach to conduct a shape-controlled synthesis of nanomaterials by focusing on pretreating the precursors and also provides an opportunity to expand the knowledge of crystal growth.

Acknowledgment. This work was supported by NSFC (20725102, 50772056), the Foundation for the Author of National Excellent Doctoral Dissertation of P. R. China, the Program for New Century Excellent Talents of the Chinese Ministry of Education, the Fok Ying Tung Education Foundation (111012), and the State Key Project of Fundamental Research for Nanoscience and Nanotechnology (2006CB932301).

Supporting Information Available: Additional figures are provided. This material is available free of charge via the Internet at http://pubs.acs.org.